- Technical Paper -

CHARACTERIZATION OF CRACK GEOMETRY IN FIRE-DAMAGED HIGH-STRENGTH CONCRETE UNDER RE-CURING USING X-RAY CT

Michael HENRY[*1], Ivan Sandi DARMA[*2] and Takafumi SUGIYAMA[*3]

ABSTRACT

This research applied X-ray microtomography and image analysis techniques to characterize the changes in crack geometry in a high-strength concrete specimen after heating at 600ºC and subsequent water re-curing up to 28 days. Results showed that cracks formed in the mortar-aggregate interface and bridged between aggregates, as well as enlarged the existing air voids. Water re-curing reduced the total crack space and a finer crack distribution could be observed after 28 days, but healing of surface cracks reduced water supply and limited healing in the inner part of the concrete.
Keywords: fire damage, water re-curing, crack geometry, crack distribution, X-ray CT

1. INTRODUCTION

Although concrete generally exhibits good fire resistance, exposure to high temperatures can lead to a reduction in overall structural performance, including decreased load-carrying capability, durability and fire resistance. These are caused by the dehydration of the cement paste as well as incompatibility in thermal expansion between the cement paste and coarse aggregates, which lead to a weakened matrix strength, coarsened pore structure, and extensive cracking. Explosive spalling has also been observed to occur in concrete materials with dense microstructures such as high-strength concrete.

Repair operations are necessary to restore performance and typically involve the removal of damaged areas and the casting of a patching material. Unfortunately, these operations require intense labor, produce waste material that must be disposed of, and consume resources in replacing the damaged areas. A repair method that utilizes the existing concrete rather than a new patching material could provide a more economical, environmentally-friendly repair option which reduces the extent of labor-intensive repairs, thus saving energy and labor costs and reducing waste generation and resource consumption.

Re-curing of fire-damaged concrete in water has been found to restore strength and durability performance through the reduction of pore space and regeneration of hydration products from the rehydration of calcium hydroxide as well as the hydration of unhydrated cement particles [1-3]. Water supply is of particular importance for recovery, as the rate of rehydration is high in such cases [4]. Furthermore, while high-strength concrete has been found to perform differently under fire loading, it has also been shown to have better recovery under re-curing due to its dense microstructure [4]. Recovery of durability has been attributed to the filling of pore space and healing of cracks as well as the consumption of calcium oxide during rehydration, which reduces the potential for harmful carbonation, but the instability of healed crack areas may limit the strength recovery [5].

As the past research works have shown that cracks play a large role in the performance loss and recovery of fire-damaged concrete, it is thus necessary to understand cracking behavior and characteristics under heating and re-curing conditions. In this paper, crack formation due to heating and crack healing under water re-curing are investigated with the objective of characterizing the effects of heating and re-curing on crack geometry. To achieve this objective, X-ray microtomography (X-ray CT) was utilized to non-destructively examine the internal structure of the fire-damaged concrete and image analysis techniques were applied to reconstruct the three-dimensional crack network and quantify its characteristics.

2. EXPERIMENTAL PROGRAM

2.1 Specimen preparation & curing

Concrete was prepared with a water-cement ratio (W/C) of 0.30 and ordinary Portland cement to achieve the properties typical of high strength concrete. After casting, cylinders (100 x 200 mm) were sealed and cured in the molds for 24 hours, then removed and placed in water curing at 20ºC for four weeks. The cylinders were then removed from water curing and 20 mm cores were extracted from the center of the cylinder. These cores were cut into 20 mm segments which were then returned to water re-curing for another nine weeks. Total curing time from casting to heating was 13 weeks in order to achieve a high degree of hydration similar to that of concrete structures in service.

*1 Assistant professor, Division of Field Engineering for the Environment, Hokkaido University, JCI Member
*2 Ph.D. student, Division of Field Engineering for the Environment, Hokkaido University, JCI Member
*3 Professor, Division of Field Engineering for the Environment, Hokkaido University, JCI Member

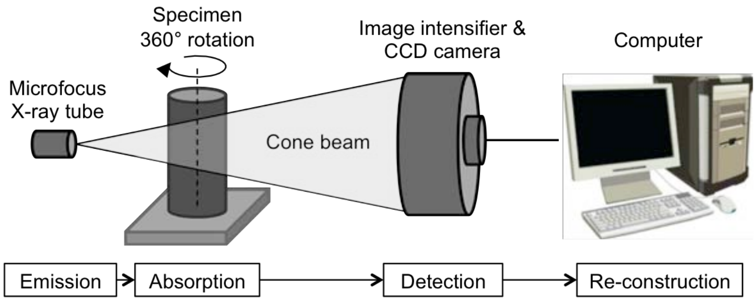

Fig. 1 Set-up for the X-ray CT image acquisition

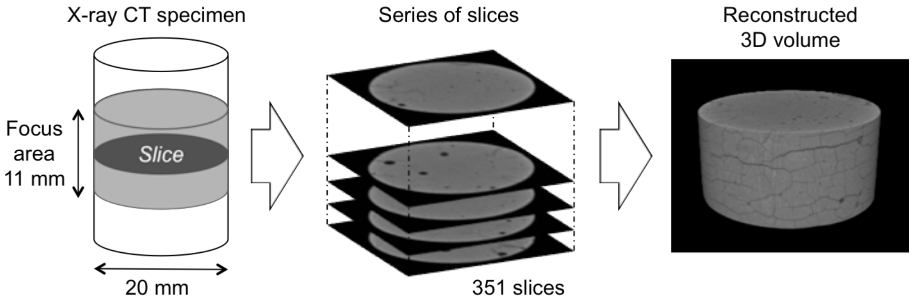

Fig. 2 Details of the X-ray CT specimen and 3D digital image reconstruction

2.2 Heating & re-curing

Fire exposure was simulated using an electric furnace with a temperature control program. The rate of heat increase was set at 10ºC per minute until the target exposure temperature of 600ºC was reached, after which it was maintained for one hour. After removal from heating, specimens were allowed to cool at room temperature for one hour then placed in water re-curing conditions similar to the initial curing period. Re-curing was carried out for four weeks.

2.3 Image acquisition using X-ray CT

As summarized by Promentilla and Sugiyama [6] and Landis and Keane [7], the concept of X-ray microtomography is similar to that of Computed Axial Tomography (CAT or CT) scans in the medical field, in which a three-dimensional (3D) digital image is reconstructed from a series of two-dimensional (2D) images or "slices." Each voxel (3D pixel) within the 3D digital image has an associated X-ray absorption value which can be correlated to material density, and thus the internal structure can be determined based on the arrangement of the voxels in a 3D space.

In this research, a desktop microfocus CT system was used for acquiring the 3D images. The set-up (Fig. 1) consists of a microfocus X-ray emitter, a rotation table, an image intensifier detector with CCD camera, and an image processing unit [8], and power settings of 130 kV and 124 μA were used for scanning. Image acquisition was carried out before heating, after heating, and after one and four weeks of water re-curing.

As illustrated in Fig. 2, the focus area was approximately 11 mm in height, 20 mm in diameter, and roughly centered on the specimen. In this area, 351 slices of 33 microns thick were obtained. Each slice was 1024 x 1024 pixels in size, with each pixel 20 x 20 microns, for a voxel size of 20 x 20 x 33 microns.

3. RESULTS & DISCUSSION

3.1 Images from before & after heating

First, the effect of heating on crack formation was examined using the cross-sectional images from before and after heating. As can be seen in Fig. 3, the heterogeneous composition of the concrete specimen makes it difficult to visually identify the formation of cracks. It should be noted that the rotation of the after-heating images relative to the before-heating images is due to the initial setting of the specimen, and there is little difference between the after-heating and after-re-curing images shown later.

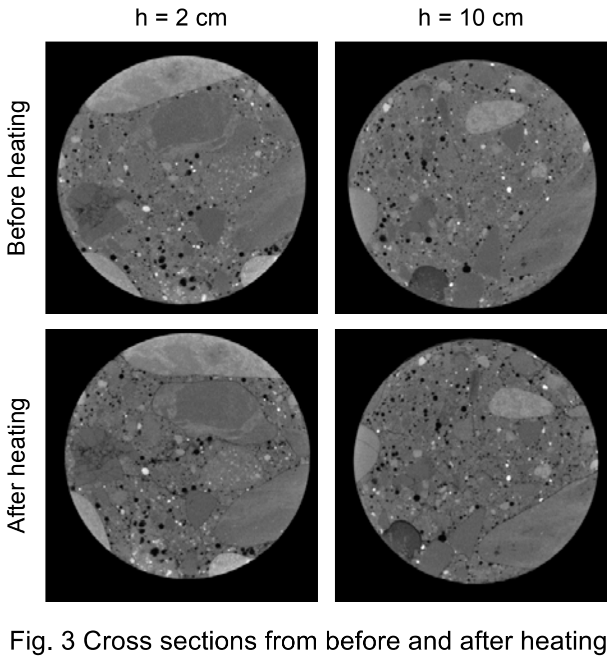

Fig. 3 Cross sections from before and after heating

3.2 Segmentation method for extracting cracks

As it was difficult to identify the cracks in the cross-sectional images by visual inspection alone, threshold segmentation was applied to clearly identify cracks in the specimen. As illustrated in Fig. 4, void space (which includes both interconnected and isolated voids) could be extracted by selecting a threshold value from the grey-scale value distribution and using that value to convert a grey-scale image to a binary black and white image. Percolated voids could then be extracted by carrying out a connectivity analysis to separate connected cracks from the isolated air voids.

3.3 Segmented images after heating & re-curing

Following the methodology illustrated in Fig. 4, the percolated void space was extracted for the entire slice image stack. Fig. 5 shows the segmented images after heating and re-curing at various heights, along with non-segmented after-heating images for reference.

After heating, cracks formed around some of the larger aggregates in the mortar-aggregate interface, most likely due to incompatibility in thermal expansion between the aggregates and the mortar. Some cracks can also be seen to bridge between different aggregates, as well as occurring within some of the aggregates themselves. Air voids within the concrete before heating (which could be seen in Fig. 3) also appeared to become enlarged and connected after heating.

The effectiveness of water re-curing for reducing the amount of percolated void space is clearly seen in the results, as after just 7 days most of the larger cracks in the mortar matrix have been healed. The remaining voids appear to be either in the interior, where it may be difficult for water to penetrate and initiate rehydration and healing, or inside the aggregates themselves, where rehydration is not possible. Two examples of cracking in aggregates can be clearly seen at the heights of 2 and 6 cm, where the percolated voids are not affected by re-curing even up to 28 days.

In addition, re-curing up to 28 days does not produce any significant reduction in the connected cracks in the interior area (particularly for h = 2 cm), supporting the hypothesis that water can no longer easily penetrate into the inner regions due to the healing of cracks in the outer area which connected the surface to the interior and provided a transport path.

3.4 Construction of 3D crack network

Three-dimensional images of the crack network after heating and re-curing were constructed from the complete segmented image stacks summarized in Fig. 5. As shown in Fig. 6, the crack network after heating can be seen to percolate in all three dimensions, with prominent semi-solid surfaces illustrating where cracks formed in the mortar-aggregate interface. It should be noted that the images are rotated so that the bottom of the specimen is facing upwards in order to highlight how the crack network formed around the aggregates.

The crack networks after 7 and 28 days of water re-curing appear to be fairly similar and, when compared with the image from after heating, the effect of water re-curing on reducing the total volume of percolated void space can be clearly observed, particularly in the lower half of the specimen.

3.5 Crack geometry characterization

Finally, quantitative measures of crack geometry were calculated to evaluate the effect of heating and re-curing on the crack network. These were carried out based on the constructed 3D volumes shown in Fig. 6.

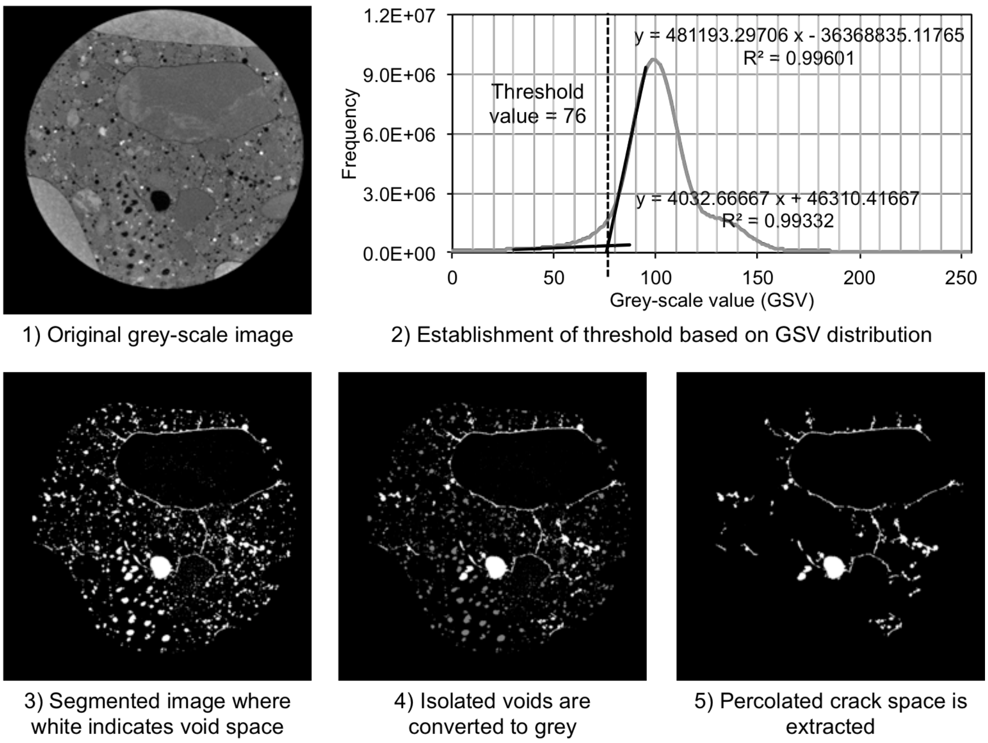

Fig. 4 Method of segmentation for extracting percolated crack space

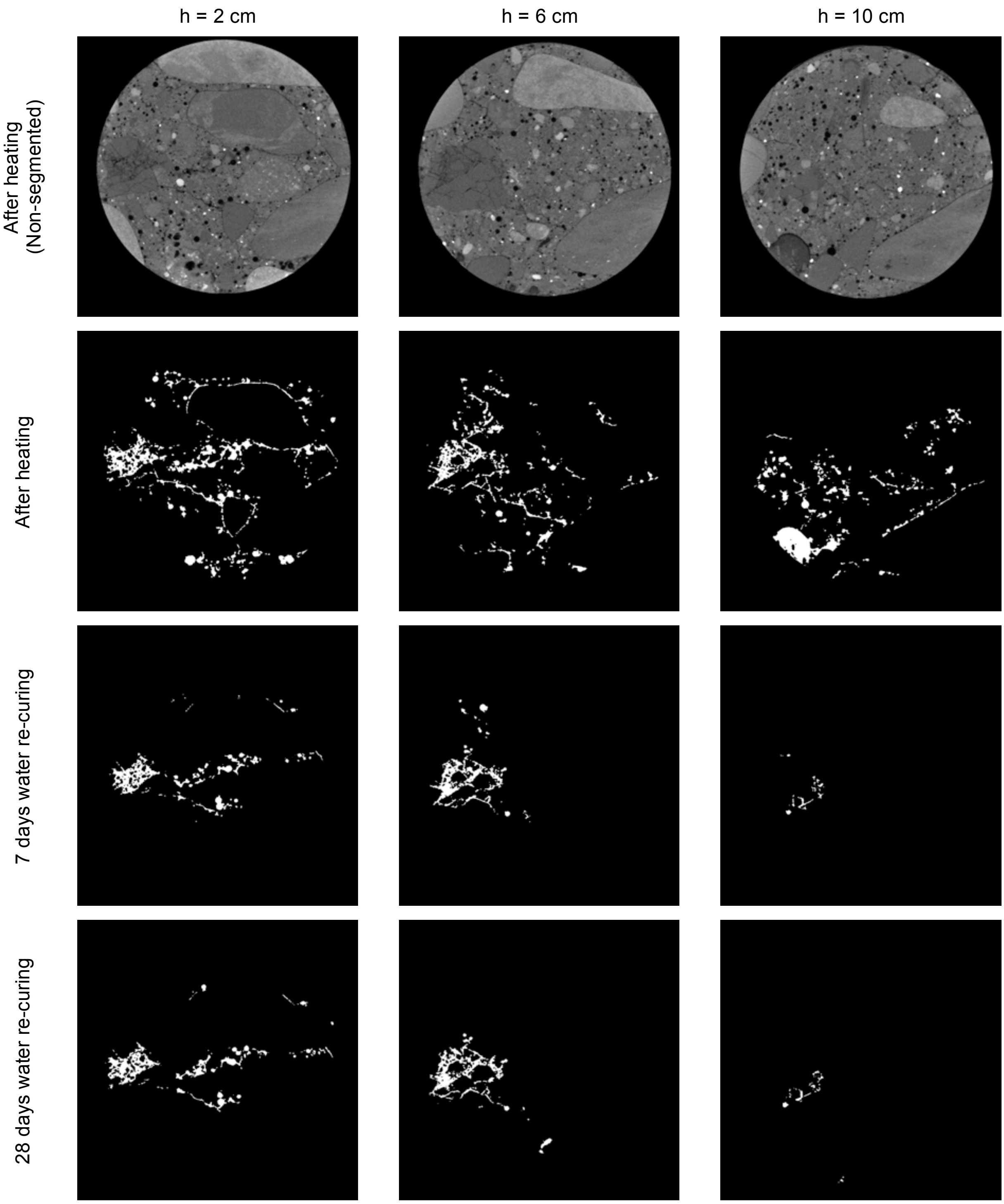

Fig. 5 Comparison of percolated void space after heating and re-curing at various heights

First, surface area, object volume, and surface to volume ratio are summarized in Table 1. The surface area of the crack network after re-curing is roughly 60% less than the surface area of the crack network after heating; however, the volume of the crack network after re-curing is only around 40% less than the volume after heating, and the surface to volume ratio after 28 days re-curing is just 30% less than that after heating. Furthermore, as greater surface to volume ratio may be an indicator of greater tortuosity, or degree of twistedness of a path, it would appear that the tortuosity of the crack network decreases after re-curing.

Second, all crack width distributions are shown in Fig. 7 along with the mean crack width for after heating and 7 and 28 days of re-curing. Mean crack width increased by about 5% after 7 days of re-curing, but the relative frequency of cracks smaller than 200 microns increased slightly relative to after heating. This trend was seen to continue for re-curing up to 28 days, where the relative frequency of smaller cracks increased even more relative to after just 7 days of water re-curing. However, the relative frequency of cracks larger than 450 microns decreased as water re-curing progressed.

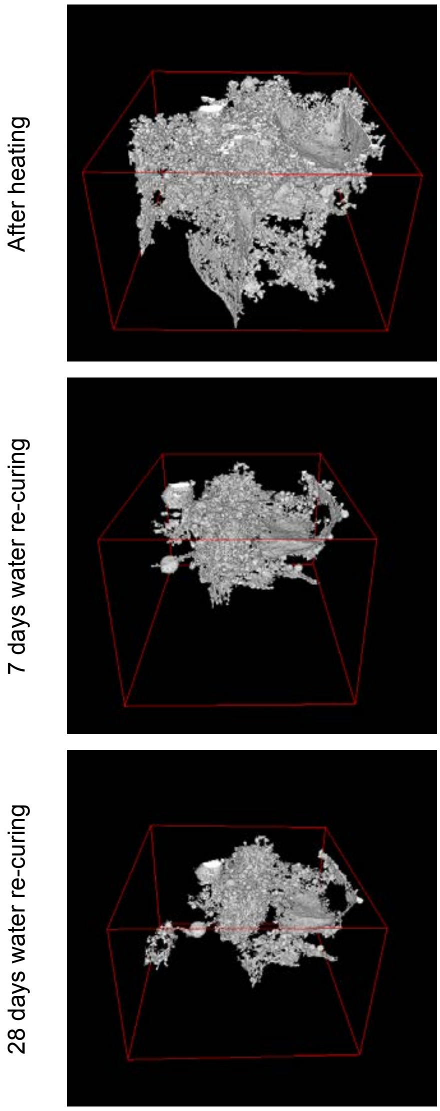

Fig. 6 Three-dimensional crack networks

Table 1 Surface and volume properties of crack networks

Surface area (m^2)	
After heating	4.76×10^{-3}
7 days water re-curing	1.98×10^{-3}
28 days water re-curing	1.96×10^{-3}
Object volume (m^3)	
After heating	1.14×10^{-7}
7 days water re-curing	7.19×10^{-8}
28 days water re-curing	6.69×10^{-8}
Surface-to-volume ratio (m^{-1})	
After heating	4.17×10^{4}
7 days water re-curing	2.75×10^{4}
28 days water re-curing	2.93×10^{4}

As a result, water re-curing was found to reduce the total volume of percolated void space and increase the relative frequency of smaller-width cracks while reducing the frequency of larger-width cracks. Crack healing can thus be seen to progress under water supply as small cracks become sealed and the width of larger cracks decreases due to the crack healing phenomenon. While this healing may possibly be attributed to rehydration of the dehydrated cement such as calcium oxide, this research does not include a concurrent analysis of the changes in chemical composition. Future research works will thus attempt to combine the observation of changes in the geometry of the crack network with such chemical analyses to fully explain the mechanism of crack healing under water re-curing.

4. CONCLUSIONS

(1) X-ray CT and image analysis techniques were applied to analyze the changes in crack geometry in high-strength concrete due to heating at 600ºC and subsequent re-curing in water.

(2) Segmentation of the 2D grey scale cross-section images based on the grey scale value distribution could allow for observation of connected cracks.

(3) Heating was observed to cause cracks in the mortar-aggregate interface due to differences in thermal expansion. Other growth in the percolated void space was due to cracks bridging between aggregates and the enlargement of pre-existing voids such as entrapped and entrained air. Aggregate cracking was also found to occur.

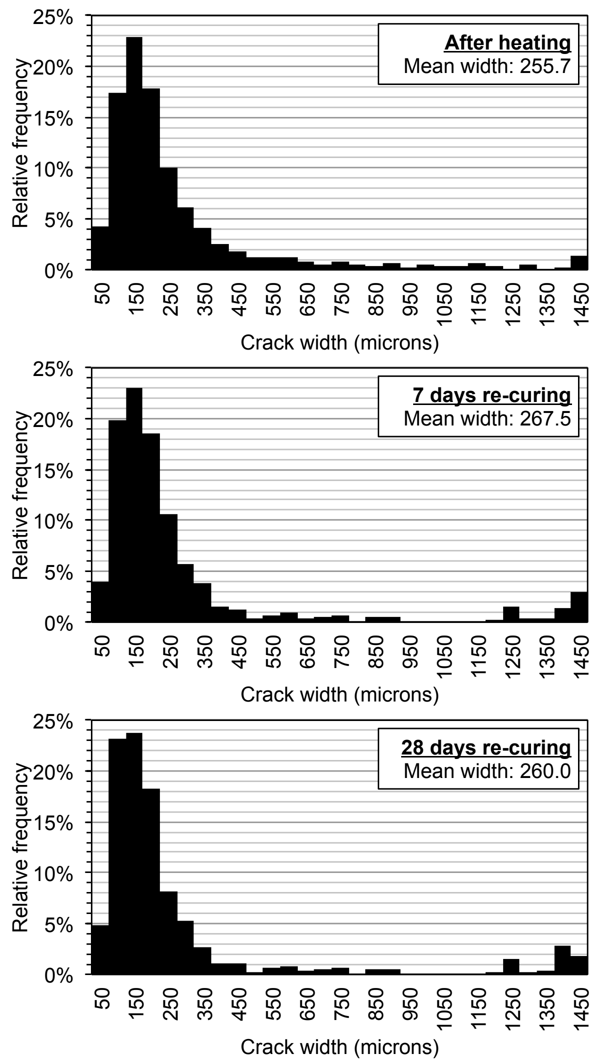

Fig. 7 Crack width distributions

(4) Water re-curing reduced the total volume of percolated void space through healing of cracks, particularly near the surface of the specimen and in some of the mortar-aggregate interfaces. However, this prevented further supply of water to voids in the inner area of the specimen, and less recovery was observed in this area. Furthermore, most of the reduction in connected cracks occurred within the first 7 days of water re-curing. No healing was observed in cracks which occurred within aggregates.

(5) The crack healing phenomenon under water re-curing could be quantitatively observed in the crack width distributions after 7 and 28 days of water re-curing, as the relative frequency of larger- width cracks was reduced and the relative frequency of smaller-width cracks increased, indicating that the crack network became finer as re-curing progressed from 7 to 28 days.

ACKNOWLEDGEMENT

This research was partially supported by the Japan Society for the Promotion of Science (Research no. 23360187).

REFERENCES

[1] Crook, D.N. and Murrary, M.J., "Regain of strength and firing of concrete," Magazine of Concrete Research 22(72), 1970, pp. 149-154.

[2] Lin, W.M., Lin, T.D., and Powers-Couche, L.J., "Microstructures of fire-damaged concrete," ACI Materials Journal 93(3), 1996, pp. 199-205.

[3] Sarshar, R. and Khoury, G.A., "Material and environmental factors influencing the compressive strength of unsealed cement paste and concrete at high temperatures," Magazine of Concrete Research 45(162), 1993, pp. 51-61.

[4] Poon, C.S., Azhar, S., Anson, M., and Wong, Y.K., "Strength and durability recovery of fire-damaged concrete after post-fire curing," Cement and Concrete Research 31, 2001, pp. 1307-1381.

[5] Henry, M., Suzuki, M., and Kato, Y., "Behavior of fire-damaged mortar under variable re-curing conditions," ACI Materials Journal 108(3), 2011, pp. 281-289.

[6] Promentilla, M.A.B. and Sugiyama, T., "X-ray microtomography of mortars exposed to freezing-thawing action," Journal of Advanced Concrete Technology 8(2), 2010, pp. 97-111.

[7] Landis, E.N. and Keane, D.T., "X-ray microtomography," Materials Characterization 61, 2010, 1305-1316.

[8] Promentilla, M.A.B., Sugiyama, T., and Shimura, K., "Three-dimensional imaging of cement-based materials with X-ray tomographic microscopy," Proc. of the Intl. Conference on Microstructure-related Durability of Cementitious Concrete, 2008, pp. 1357-1366.